J Opt
https://doi.org/10.1007/s12596-024-01709-0

RESEARCH ARTICLE

Analyzing electron acceleration mechanisms in magnetized plasma using Sinh–Gaussian pulse excitation

Vivek Sharma[1] · **Vishal Thakur**[1]

Received: 26 December 2023 / Accepted: 31 January 2024

Abstract The phenomenon of laser wakefield acceleration is one of the prominent mechanisms to accelerate electrons to very high energies within a very small propagation distance. In this study, we have chosen Sinh–Gaussian laser pulse with static magnetic field perpendicular to direction of propagation of pulse. Analytical solution for chosen electric field is obtained from a generalized differential equation of laser wake potential. Hence, expressions for wakefield and electron energy gain are also obtained. Using feasible parameters, it is observed that when laser field amplitude increases from 3.85×10^{11} to 4.81×10^{11} V/m, electron energy gain increases from 102.504 to 160.163 MeV in the absence of external magnetic field and 103.258 to 160.918 MeV in an external magnetic field of 40 T. So, laser field amplitude and strength of magnetic field both have direct impact on electron energy gain and enhance in energy gain can be seen. Our research will be useful for the researchers to obtain a more energy efficient electron acceleration mechanism.

Keywords Laser wakefield acceleration · Sinh–Gaussian laser pulse · Magnetic field strength · Electron energy gain · Energy efficiency

Introduction

Laser plasma interaction is a widely used phenomenon for producing various nonlinear effects like production of various radiations of desired frequency (THz generation [1–10] and harmonic generation [11–17]), controlling the intensity of propagating laser pulse (self-focusing [18–23]), particle acceleration (laser wakefield acceleration [24–27] and plasma wake field acceleration [28, 29]), etc. Particle acceleration, especially electron acceleration is one of the most important utilized nonlinear phenomena. Optimization of various laser and plasma parameters is required for the maximum energy efficient laser wakefield acceleration (LWFA). Askari et al. [30] have compared LWFA produced by Gaussian-like and rectangular–triangular pulse in magnetized plasma. In this study, they have investigated the role of pulse profile along with the role of external magnetic field. Abedi-Varaki et al. [31] have taken Gaussian, super-Gaussian, and Bessel–Gaussian profile for the comparative study of LWFA in magnetized plasma. Role of laser pulse profile on LWFA using different Gaussian-like laser pulses is investigated by Sharma et al. [32] and found that the laser pulse with broadest pulse profile is most suited for wakefield generation.

The role of frequency chirped laser pulse (both positive and negative) on electron acceleration is investigated by Ghotra [33], Pathak et al. [34], Zhang et al. [35], Sharma et al. [36, 37], Jain et al. [38] and Singh et al. [39]. Role of laser pulse polarization is investigated by Heydarzadeh et al. [40], Sharma et al. [41], and Zhang et al. [42]. Plasma density also plays a crucial role in electron acceleration process. Sharma et al. [43] have studied plasma with ripple density variation, and Pukhov et al. [44] and Gupta et al. [45] have investigated LWFA in density modulated plasma. Up-ramp density plasma has positive correlation with electron energy gain in LWFA [46].

Asymmetric laser pulse can significantly affect electron acceleration due to its specific pulse shape. Leemans et al. [47], Sharma et al. [48], Xie et al. [49], Gopal et al. [50], etc. have investigated this correlation. Sharma et al. [51]

✉ Vishal Thakur
vishal20india@yahoo.co.in

[1] Department of Physics, Lovely Professional University, G.T. Road, Phagwara, , Punjab 144411, India

have studied the role of wiggler magnetic field, Abedi-Varaki [52] have selected periodic magnetic field, and Singh et al. [53] have used sheared magnetic field to investigate their role on laser wakefield acceleration. The effect of beating of laser pulses to enhance wakefield excitation is investigated by Sharma et al. [54].

In this study, we have chosen Sinh–Gaussian pulse profile with transverse static magnetic field to investigate the role of both chosen laser profile and magnetic field. Using this specific pulse profile, analytical solution for wake potential, wakefield and electron energy gain is derived in section II. By selecting feasible parameters, curves are drawn in result and discussion section III. Research outcomes based on these curves are discussed in conclusion section IV. The paper ends with references.

Derivation of formulas

A laser pulse with an electric field E and a magnetic field B that is traveling in the z-direction through a uniform plasma with a density n is analyzed. The rest mass of an electron is denoted as m_0. We introduce a new parameter, defined as $\xi = z - v_g t$, where v_g represents the group velocity and t is the time. An external magnetic field, denoted as B_0, is applied in the y-direction. The expression for the wake potential (Φ) created in the presence of an external transverse magnetic field is as follows: [32]

$$\left(\frac{\partial^2\Phi}{\partial\xi^2}\right) + k_P^2\Phi - \left\{\frac{e\left(\beta^2-1\right)}{2m_0 v_g^2}\right\}\left(E^2 + 2B_0 E v_g\right) = 0 \quad (1)$$

Here, β is the ratio of speed of light in vacuum to group velocity. $\beta = c/v_g$, and $k_P \times v_g = \omega_P$.

In this study, we have chosen a Sinh–Gaussian laser pulse with a pulse envelope expressed as

$$E^2 = E_0^2 e^{-\frac{2\left(\xi-\frac{L}{2}\right)^2}{w_0^2}}\left\{\sinh\left(\frac{\left(\xi-\frac{L}{2}\right)}{w_0}\right)\right\}^2, \ 0 \le \xi \le L \quad (2)$$

Here, w_0 indicates the laser's characteristics, E_0 represents the strength of the laser's electric field, and L represents the length of the pulse.

By solving Eq. (1) for the laser profile described in Eq. (2), we derive the resulting wake potential:

$$\begin{aligned}
\Phi = {} & \frac{1}{8k_P m_0 v_g} iee^{\frac{1}{4}\left(1-k_P^2 w_0^2-2ik_P\left(L+2\xi+w_0\right)\right)}\left(e^{iLk_P}+e^{2i\xi k_P}\right)\sqrt{\pi} \\
& (-1+\beta^2)\Bigg(e^{ik_P w_0} erf\left[\frac{1}{2}\left(-1+\frac{L}{w_0}-ik_P w_0\right)\right] - erf\left[\frac{1}{2}\left(-1+\frac{L}{w_0}+ik_P w_0\right)\right] \\
& -erf\left[\frac{L+w_0-ik_P w_0^2}{2w_0}\right] + e^{ik_P w_0} erf\left[\frac{L+w_0+ik_P w_0^2}{2w_0}\right]\Bigg)B_0 w_0 \mathbb{E}_0 \\
& + \frac{1}{32k_P m_0 v_g^2} ee^{-\frac{1}{8}k_P\left(4i(L+2\xi)+4iw_0+k_P w_0^2\right)}\left(e^{iLk_P}-e^{2i\xi k_P}\right)\sqrt{\frac{\pi}{2}} \\
& (-1+\beta^2)\Bigg(ie^{\frac{1}{2}+ik_P w_0} erf\left[\frac{2L+2w_0+ik_P w_0^2}{2\sqrt{2}w_0}\right] + 2e^{\frac{1}{2}ik_P w_0} erfi\left[\frac{-2iL+k_P w_0^2}{2\sqrt{2}w_0}\right] - 2e^{\frac{1}{2}ik_P w_0} erfi\left[\frac{2iL+k_P w_0^2}{2\sqrt{2}w_0}\right] \\
& + e^{\frac{1}{2}+ik_P w_0} erfi\left[\frac{2iL-2iw_0+k_P w_0^2}{2\sqrt{2}w_0}\right] - \sqrt{e} erfi\left[\frac{-2iL+2iw_0+k_P w_0^2}{2\sqrt{2}w_0}\right] \\
& + \sqrt{e} erfi\left[\frac{2iL+2iw_0+k_P w_0^2}{2\sqrt{2}w_0}\right]\Bigg) w_0 \mathbb{E}_0^2
\end{aligned} \quad (3)$$

The formula for generated longitudinal laser wakefield is $E_w = -\frac{\partial \Phi}{\partial z}$

$$
\begin{aligned}
E_w = &-\frac{1}{64 m_0 v_g^2} \mathrm{e} e^{-\frac{1}{8}k_P\left(8i(L+2\xi)+w_0\left(8i+3k_P w_0\right)\right)}\sqrt{\pi} \\
&(-1+\beta^2) w_0 \mathbb{E}_0 \Big(8 e^{\frac{1}{8}\left(2+k_P^2 w_0^2+4ik_P\left(L+2\xi+w_0\right)\right)}\left(e^{iLk_P}-e^{2i\xi k_P}\right) \\
&\left(-2+e^{ik_P w_0}\left(\mathrm{erf}\left[\frac{1}{2}\left(-1+\frac{L}{w_0}-ik_P w_0\right)\right]+\mathrm{erf}\left[\frac{1}{2}\left(1+\frac{L}{w_0}+ik_P w_0\right)\right]\right)\right. \\
&\left.+\mathrm{erfc}\left[\frac{1}{2}\left(1+\frac{L}{w_0}-ik_P w_0\right)\right]+\mathrm{erfc}\left[\frac{1}{2}\left(-1+\frac{L}{w_0}+ik_P w_0\right)\right]\right) B_0 v_g \\
&-\sqrt{2} e^{\frac{1}{4}k_P\left(2i(L+2\xi)+w_0\left(2i+k_P w_0\right)\right)}\left(e^{iLk_P}+e^{2i\xi k_P}\right)\Bigg(2e^{\frac{1}{2}ik_P w_0}\left(\mathrm{erf}\left[\frac{2L-ik_P w_0^2}{2\sqrt{2}w_0}\right]+\mathrm{erf}\left[\frac{2L+ik_P w_0^2}{2\sqrt{2}w_0}\right]\right) \\
&+\sqrt{e}\left(\mathrm{erf}\left[\frac{-2L+w_0\left(2-ik_P w_0\right)}{2\sqrt{2}w_0}\right]-\mathrm{erf}\left[\frac{2L+w_0\left(2-ik_P w_0\right)}{2\sqrt{2}w_0}\right]\right) \\
&+e^{\frac{1}{2}+ik_P w_0}\left(\mathrm{erf}\left[\frac{-2L+w_0\left(2+ik_P w_0\right)}{2\sqrt{2}w_0}\right]-\mathrm{erf}\left[\frac{2L+w_0\left(2+ik_P w_0\right)}{2\sqrt{2}w_0}\right]\right)\Bigg)\mathbb{E}_0\Big)
\end{aligned} \tag{4}
$$

The error function (erf) and the imaginary error function (erfi) are defined in this context as follows: [55]

$\mathrm{erf}\,[Y] = \frac{2}{\sqrt{\pi}}\int_0^Y e^{-q^2}\mathrm{d}q$, $\mathrm{erfc}\,[Y] = 1 - \mathrm{erf}[Y]$ and $\mathrm{erfi}\,[Y] = \frac{2}{\sqrt{\pi}}\int_0^Y e^{q^2}\mathrm{d}q$, respectively.

For a new variable $\eta = k_p(\xi - L/2)$, the change in the relativistic factor ($\Delta\gamma$) is

$$
\Delta\gamma = \frac{-e}{k_p m_0 c^2\left\{1-\frac{1}{\beta}\right\}}\int E_w \mathrm{d}\eta
$$

By utilizing the formula, one can obtain the energy gained by an electron called electron energy gain. $\Delta W = m_0 c^2 \Delta\gamma$.

$$
\begin{aligned}
\Delta W = &\frac{e}{64(-1+\beta)k_P m_0 v_g^2}\mathrm{ie}\left(-1+e^{i\xi k_P}\right)\sqrt{\pi}\beta \\
&(-1+\beta^2) w_0 \mathbb{E}_0 \Big(-8 e^{\frac{1}{4}-\frac{1}{4}k_P^2 w_0^2-ik_P\left(L+\xi+w_0\right)}\left(e^{\frac{1}{2}ik_P\left(3L+w_0\right)}-e^{\frac{1}{2}ik_P\left(L+2\xi+w_0\right)}\right) \\
&\left(-2+e^{ik_P w_0}\left(\mathrm{erf}\left[\frac{1}{2}\left(-1+\frac{L}{w_0}-ik_P w_0\right)\right]+\mathrm{erf}\left[\frac{1}{2}\left(1+\frac{L}{w_0}+ik_P w_0\right)\right]\right)\right. \\
&\left.+\mathrm{erfc}\left[\frac{1}{2}\left(1+\frac{L}{w_0}-ik_P w_0\right)\right]+\mathrm{erfc}\left[\frac{1}{2}\left(-1+\frac{L}{w_0}+ik_P w_0\right)\right]\right) B_0 v_g \\
&+\sqrt{2} e^{-\frac{1}{8}k_P\left(4i(L+2\xi)+w_0\left(4i+k_P w_0\right)\right)}\left(e^{iLk_P}+e^{i\xi k_P}\right)\Bigg(2e^{\frac{1}{2}ik_P w_0}\Big(\mathrm{erf}\left[\frac{2L-ik_P w_0^2}{2\sqrt{2}w_0}\right] \\
&+\mathrm{erf}\left[\frac{2L+ik_P w_0^2}{2\sqrt{2}w_0}\right]\Big)+\sqrt{e}\left(\mathrm{erf}\left[\frac{-2L+w_0\left(2-ik_P w_0\right)}{2\sqrt{2}w_0}\right]-\mathrm{erf}\left[\frac{2L+w_0\left(2-ik_P w_0\right)}{2\sqrt{2}w_0}\right]\right) \\
&+e^{\frac{1}{2}+ik_P w_0}\left(\mathrm{erf}\left[\frac{-2L+w_0\left(2+ik_P w_0\right)}{2\sqrt{2}w_0}\right]-\mathrm{erf}\left[\frac{2L+w_0\left(2+ik_P w_0\right)}{2\sqrt{2}w_0}\right]\right)\Bigg)\mathbb{E}_0\Big)
\end{aligned} \tag{5}
$$

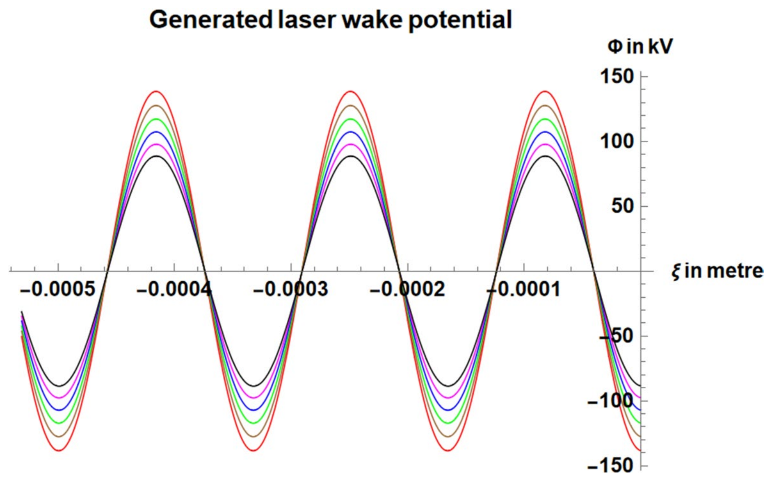

Fig. 1 Illustration of generated laser wake potential with propagation distance for laser electric field 3.85×10^{11} V/m (black), 4.04×10^{11} V/m (magenta) 4.23×10^{11} V/m (blue), 4.43×10^{11} V/m (green), 4.61×10^{11} V/m (brown), and 4.81×10^{11} V/m(red). $B_0 = 20\ T$, w_0= 16.87 µm, L = 83 µm

Result and discussion

The current study utilized plasma with the following specifications: an electron density of 4×10^{22} m^{-3}, a frequency of 1.13×10^{13} rad/s, and plasma wavelength of 166 µm corresponding to selected plasma density. In the numerical investigation, a laser pulse was chosen with a wavelength of 10.6 µm (generated by CO_2 laser source), a frequency of 1.78×10^{14} rad/s, and a pulse duration of 83 µm. The selected amplitudes of the laser electric field (E_0) are 3.85×10^{11} V/m, 4.04×10^{11} V/m, 4.23×10^{11} V/m, 4.43×10^{11} V/m, 4.61×10^{11} V/m, and 4.81×10^{11} V/m. The numerical value of w_0 is 16.87 µm. To assess the influence of the magnetic field on electron acceleration via the LWFA phenomenon, we employ external field intensities of 0, 10, 20, 30, and 40 T (1 T = 10 kilogauss).

Figure 1 illustrates the variation of generated laser wake potential with propagation distance for different laser intensities. With the increase in laser intensity from 3.85×10^{11} to 4.81×10^{11} V/m, amplitude of generated wake potential increases from 88.7471 to 138.581 kV for static magnetic field of 20 T. Curves are plotted to obtain peak values of generated wake potential for selected different laser pulse amplitude at external magnetic field strength 0 T, 10 T, 20 T, 30 T, and 40 T. The peak values of generated wake potential are noted in Table 1. Using these data, Fig. 2 is plotted to show the variation of generated wake potential with laser electric field amplitude of 3.85×10^{11} V/m and selected magnetic field. Curve represents a positive correlation of generated wake potential with external magnetic field.

Figure 3 depicts the relationship between the laser intensities and the generated laser wakefield as the propagation distance changes. By increasing the laser intensity from 3.85×10^{11} to 4.81×10^{11} V/m, the amplitude of the generated wakefield increases from 3.89 to 6.08 GV/m. This occurs when a static magnetic field of 20 T is applied. Laser wakefield graphs are generated for various laser pulse

Table 1 Amplitude of generated wake potential (in kV) with laser field amplitude (E_0) and external magnetic field strength (B_0)

E_0 (V/m)	B_0				
	0 T	10 T	20 T	30 T	40 T
3.85×10^{11}	88.5944	88.6326	88.7471	88.9377	89.2037
4.04×10^{11}	97.6753	97.7135	97.828	98.0186	98.2849
4.23×10^{11}	107.199	107.237	107.352	107.543	107.809
4.43×10^{11}	117.166	117.204	117.319	117.509	117.776
4.61×10^{11}	127.576	127.614	127.729	127.919	128.186
4.81×10^{11}	138.429	138.467	138.581	138.772	139.039

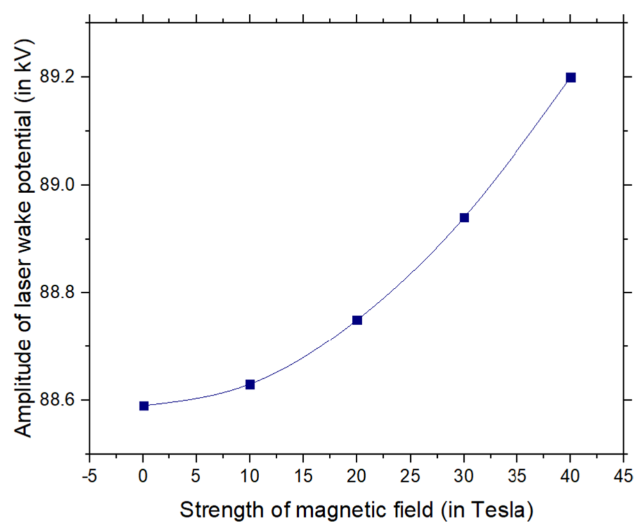

Fig. 2 Illustration of generated laser wake potential amplitude for different magnetic field strength w_0= 16.87 µm, L = 83 µm and laser field amplitude 3.85×10^{11} V/m

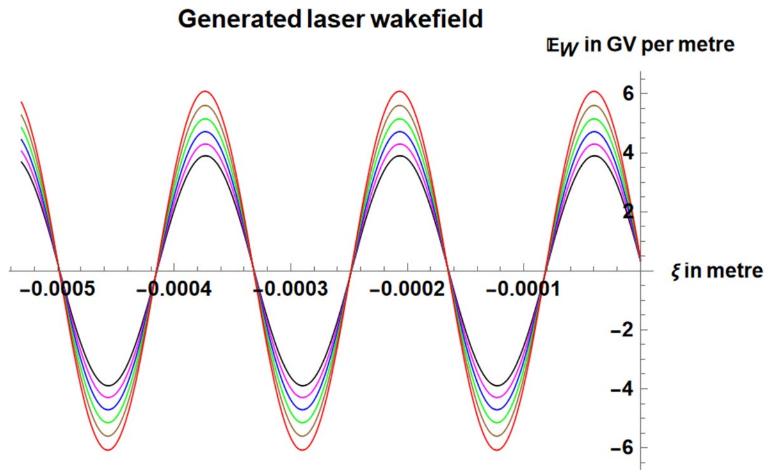

Fig. 3 Illustration of generated laser wakefield with propagation distance for laser electric field 3.85×10^{11} V/m(black), $4.04 \times, 10^{11}$ V/m(magenta) 4.23×10^{11} V/m(blue), 4.43×10^{11} V/m (green), $.61 \times 10^{11}$ V/m (brown), and 4.81×10^{11} V/m (red). $B_0 = 20T$, w_0= 16.87 µm, L = 83 µm

Table 2 Amplitude of generated wakefield (in GV/m) with laser field amplitude (E_0) and external magnetic field strength (B_0)

E_0 (V/m)	B_0				
	0 T	10 T	20 T	30 T	40 T
3.85×10^{11}	3.88469	3.88828	3.89903	3.9169	3.94177
4.04×10^{11}	4.28287	4.28646	4.29722	4.31509	4.33999
4.23×10^{11}	4.70047	4.70406	4.71482	4.7327	4.75762
4.43×10^{11}	5.1375	5.14109	5.15185	5.16974	5.19468
4.61×10^{11}	5.59395	5.59754	5.6083	5.6262	5.65115
4.81×10^{11}	6.06982	6.07341	6.08418	6.10208	6.12705

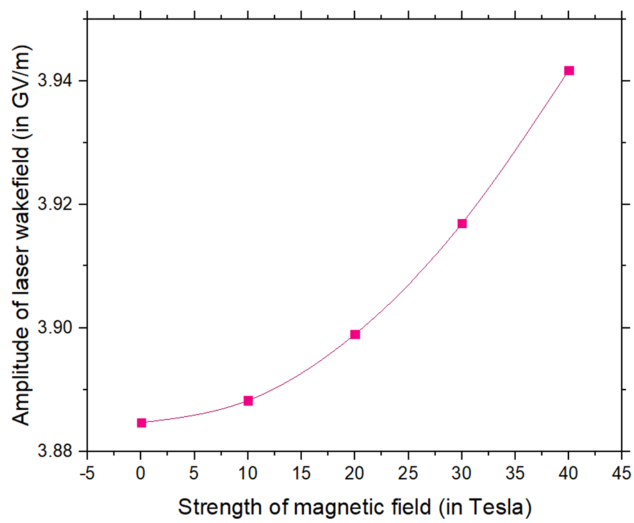

Fig. 4 Illustration of generated laser wakefield amplitude for different magnetic field strength w_0= 16.87 µm, L = 83 µm and laser field amplitude 3.85×10^{11} V/m

amplitudes and external magnetic field strengths of 0 T, 10 T, 20 T, 30 T, and 40 T. The maximum value of the generated wakefield is shown in Table 2. Based on the provided data, Fig. 4 illustrates the relationship between the generated wakefield and magnetic field for the laser electric field amplitude of 3.85×10^{11} V/m. The curve illustrates a direct relationship between the generated wakefield and the external magnetic field.

The relationship between the electron energy gain and propagation distance for various laser intensities is shown in Fig. 5. The maximum energy gain increases from 102.694 to 160.353 MeV as the laser intensity rises from 3.85×10^{11} to 4.81×10^{11} V/m in a static magnetic field of 20 T. Curves are generated to represent specific variations in electron energy gain in response to laser pulse amplitude and external magnetic field strengths of 0 T, 10 T, 20 T, 30 T, and 40 T. Table 3 presents the maximum value of the electron energy gain amplitude that was generated. Based on the provided data, Fig. 6 illustrates the correlation between the generated wake potential and the chosen magnetic field at constant laser electric field amplitude of 3.85×10^{11} V/m. The curve illustrates a positive correlation between the electron energy gain and the external magnetic field.

When an intense laser beam propagates through underdense plasma, nonlinear ponderomotive force and electrostatic force between electron and positive ions are responsible for periodic oscillation of electrons (plasma wave) about the axis of propagation of laser pulse. As a result, a wake potential and wakefield develops along the longitudinal axis called laser wake potential and laser wakefield, respectively, which can be utilized to accelerate electrons. With the increase in laser field amplitude or strength of external magnetic field, the phenomenon of electron acceleration becomes more effective. It can be seen through the curves obtained in our study.

Using Gaussian-like and rectangular–triangular pulses, Askari et al. [30] have studied the impact of magnetic field on wakefield generation and concluded that the use of

Fig. 5 Illustration of electron energy gain with propagation distance for laser electric field 3.85×10^{11} V/m(black), 4.04×10^{11} V/m(magenta) 4.23×10^{11} V/m(blue), 4.43×10^{11} V/m (green), 4.61×10^{11} V/m(brown), and 4.81×10^{11} V/m(red). $B_0 = 20T$, w_0= 16.87 µm, L = 83 µm

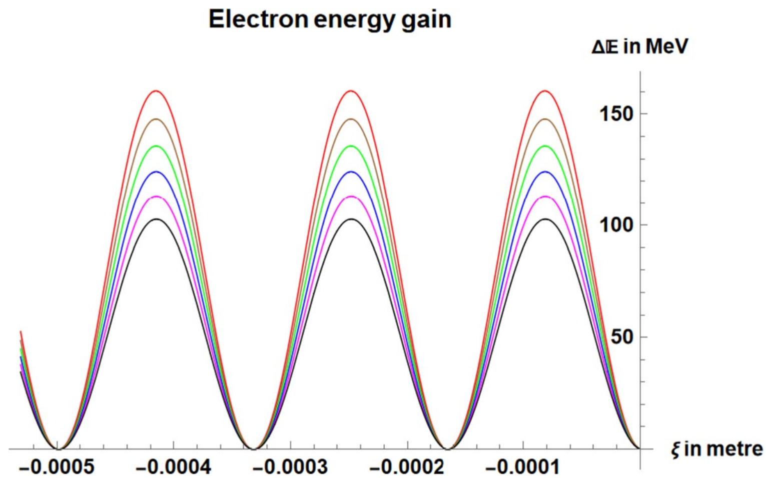

Table 3 Amplitude of electron energy gain (in MeV) with laser field amplitude (E_0) and external magnetic field strength (B_0)

E_0 (V/m)	B_0				
	0 T	10 T	20 T	30 T	40 T
3.85×10^{11}	102.504	102.552	102.694	102.929	103.258
4.04×10^{11}	113.011	113.059	113.2	113.436	113.765
4.23×10^{11}	124.03	124.078	124.22	124.456	124.784
4.43×10^{11}	135.562	135.609	135.751	135.987	136.317
4.61×10^{11}	147.606	147.654	147.796	148.032	148.361
4.81×10^{11}	160.163	160.211	160.353	160.589	160.918

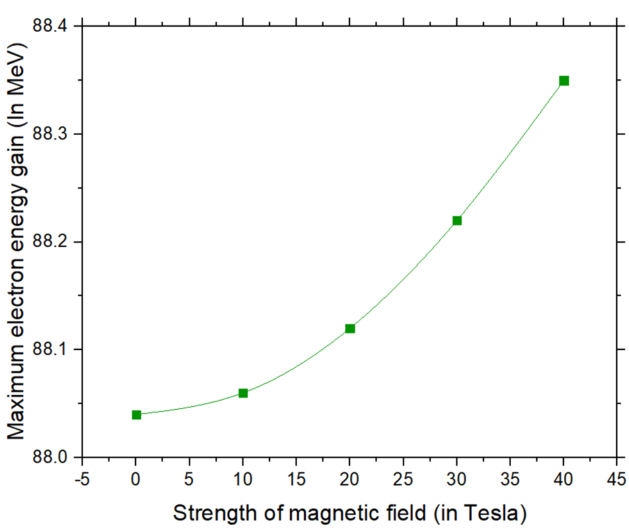

Fig. 6 Illustration of maximum electron energy gain for different magnetic field strength w_0= 16.87 µm, L = 83 µm and laser field amplitude 3.85×10^{11} V/m

external magnetic field enhances acceleration of electrons. They also used Gaussian laser pulse for the similar study [56].

Conclusion

Laser wakefield acceleration (LWFA) is a notable process that rapidly increases the energy of electrons over a short distance using laser-induced wakefield. For this investigation, we have selected a Sinh–Gaussian laser pulse that is accompanied by a static magnetic field positioned perpendicular to the pulse's direction of propagation. The analytical solution for the selected electric field is derived from a generalized differential equation of the laser wake potential. Consequently, equations for the wakefield and the increase in electron energy are also derived. By varying the laser field amplitude within reasonable limits, it was found that increasing it from 3.85×10^{11} to 4.81×10^{11} V/m resulted in an increase in electron energy gain from 102.504 to 160.163 MeV when there was no external magnetic field. When an external magnetic field of 40 T was present, the electron energy gain increased from 103.258 to 160.918 MeV. The amplitude of the laser field and the strength of the magnetic field directly affect the increase in electron energy gain, resulting in an enhancement of energy gain. Out of electric and magnetic fields, the role of electric field is dominant as per the results of our study using selected parameters. An electric field of high amplitude can enhance the wakefield more effectively to generate a plasma wave of higher amplitude. This generated plasma wave is responsible for generating enhanced laser wakefield acceleration. Our findings will provide valuable insights for researchers seeking to enhance the efficiency of electron acceleration mechanisms for energy production.

Author contributions VS involved in derivation, methodology, analytical modeling, graph plotting, and result discussion; VT involved in supervision, reviewing, and editing.

Funding Not applicable.

Data availability The data that support the findings of this study are available from the corresponding authors upon reasonable request.

Declarations

Conflict of interest The authors declare no competing interest.

Ethics approval Not applicable.

Consent to participate Not applicable.

Consent for publication Not applicable.

References

1. M. Singh, R.K. Singh, R.P. Sharma, THz generation by cosh-Gaussian lasers in a rippled density plasma. EPL (Europhys. Lett.) **104**(3), 35002 (2013)
2. H.K. Midha, V. Sharma, N. Kant, V. Thakur, Efficient THz generation by Hermite-cosh-Gaussian lasers in plasma with slanting density modulation. J. Opt. (2023). https://doi.org/10.1007/s12596-023-01413-5
3. H.K. Midha, V. Sharma, N. Kant, V. Thakur, Resonant Terahertz radiation by p-polarised chirped laser in hot plasma with slanting density modulation. J. Opt. (2023). https://doi.org/10.1007/s12596-023-01563-6
4. V. Thakur, N. Kant, S. Kumar, THz field enhancement under the influence of cross-focused laser beams in the m-CNTs. Trends Sci. **20**(6), 5284 (2023)
5. S. Kumar, S. Vij, N. Kant, V. Thakur, Combined effect of transverse electric and magnetic fields on THz generation by beating of two amplitude-modulated laser beams in the collisional plasma. J. Astrophys. Astron. **43**(1), 30 (2022)
6. S. Kumar, S. Vij, N. Kant, V. Thakur, (2022) Interaction of obliquely incident lasers with anharmonic CNTs acting as dipole antenna to generate resonant THz radiation. Waves Random Complex Med. (2022). https://doi.org/10.1080/17455030.2022.2155330
7. S. Kumar, S. Vij, N. Kant, V. Thakur, Resonant terahertz generation by the interaction of laser beams with magnetized Anharmonic carbon nanotube array. Plasmonics **17**(1), 381–388 (2022)
8. S. Kumar, S. Vij, N. Kant, V. Thakur, Resonant terahertz generation by cross-focusing of Gaussian laser beams in the array of vertically aligned anharmonic and magnetized CNTs. Opt. Commun. **513**, 128112 (2022)
9. S. Kumar, V. Thakur, N. Kant, Magnetically enhanced THz generation by self-focusing laser in VA-MCNTs. Phys. Scr. **98**(8), 085506 (2023)
10. S. Kumar, N. Kant, V. Thakur, Magnetically tuned THz radiation through the HA-HA-CNTs under the effect of a transverse electric field. Indian J. Phys. (2023). https://doi.org/10.1007/s12648-023-02849-y
11. M. Singh, D.N. Gupta, Relativistic third-harmonic generation of a laser in a self-sustained magnetized plasma channel. IEEE J. Quantum Electron. **50**(6), 491–496 (2014)
12. V. Sharma, V. Thakur, A. Singh, N. Kant, Third harmonic generation of a relativistic self-focusing laser in plasma under exponential density ramp. Z. Naturfr. Sect. J. Phys. Sci. **77**(4), 323–328 (2022)
13. S. Sohrabi, S. Jelvani, K. Samavati, L. Farhang Matin, Effect of chirp parameter on the second harmonic efficiency in relativistic super-Gaussian laser-plasma interaction. Opt. Quantum Electron **55**(11), 942 (2023)
14. H.K. Dua, N. Kant, V. Thakur, Second harmonic generation induced by a surface plasma wave on a metallic surface in the presence of a wiggler magnetic field. Braz. J. Phys. **52**(2), 44 (2022)
15. N. Kant, A. Singh, V. Thakur, Second-harmonic generation by a chirped laser pulse with the exponential density ramp profile in the presence of a planar magnetostatic wiggler. Laser Part. Beams **37**(4), 442–447 (2019)
16. V. Thakur, N. Kant, Optimization of wiggler wave number for density transition based second harmonic generation in laser plasma interaction. Optik (Stuttg) **142**, 455–462 (2017)
17. V. Thakur, N. Kant, Resonant second harmonic generation in plasma under exponential density ramp profile. Optik (Stuttg) **168**, 159–164 (2018)
18. N. Gupta, S. Kumar, S.B. Bhardwaj, Stimulated Raman scattering of self-focused elliptical q-Gaussian laser beam in plasma with axial density ramp: effect of ponderomotive force. J. Opt. **51**(4), 819–833 (2022)
19. S. Kumar, N. Kant, V. Thakur, THz generation by self-focused Gaussian laser beam in the array of anharmonic VA-CNTs. Opt Quantum Electron **55**(3), 281 (2023)
20. V. Thakur, S. Kumar, N. Kant, Self-focusing of a Bessel-Gaussian laser beam in plasma under density transition. J. Nonlinear Opt. Phys. Mater. (2022). https://doi.org/10.1142/S0218863523500388
21. V. Thakur, N. Kant, Stronger self-focusing of cosh-Gaussian laser beam under exponential density ramp in plasma with linear absorption. Optik (Stuttg) **183**, 912–917 (2019)
22. V. Thakur, M. Ahmad Wani, N. Kant, Relativistic self-focusing of Hermite-cosine-Gaussian laser beam in collisionless plasma with exponential density transition. Commun. Theor. Phys. **71**(6), 736–740 (2019)
23. V. Thakur, N. Kant, Combined effect of chirp and exponential density ramp on relativistic self-focusing of Hermite-Cosine-Gaussian laser in Collisionless cold quantum plasma. Braz. J. Phys. **49**(1), 113–118 (2019)
24. T. Tajima, J.M. Dawson, Laser electron accelerator. Phys. Rev. Lett. **43**, 267 (1979)
25. T. Tajima, X.Q. Yan, T. Ebisuzaki, Wakefield acceleration. Rev. Mod. Plasma. Phys. **4**(1), 7 (2020)
26. V. Sharma, V. Thakur, Enhanced laser wakefield acceleration utilizing Hermite-Gaussian laser pulses in homogeneous plasma. J. Opt. (2023). https://doi.org/10.1007/s12596-023-01565-4
27. V. Sharma, N. Kant, V. Thakur, Electron acceleration in collisionless plasma: comparative analysis of laser wakefield acceleration using Gaussian and cosh-squared-Gaussian laser pulses. J. Opt. (2024). https://doi.org/10.1007/s12596-023-01564-5
28. S. Afhami, E. Eslami, Effect of nonlinear chirped Gaussian laser pulse on plasma wake field generation. AIP Adv. (2014). https://doi.org/10.1063/1.4894452
29. H. Akou, M. Asri, Dependence of plasma wake wave amplitude on the shape of Gaussian chirped laser pulse propagating in a plasma channel. Phys. Lett. A **380**(20), 1729–1734 (2016)
30. H.R. Askari, A. Shahidani, Effect of magnetic field on production of wake field in laser–plasma interactions: Gaussian-like (GL) and

rectangular–triangular (RT) pulses. Opt. Int. J. Light Electron Opt. **124**(17), 3154–3161 (2013)
31. M. Abedi-Varaki, N. Kant, Magnetic field-assisted wakefield generation and electron acceleration by Gaussian and super-Gaussian laser pulses in plasma. Mod. Phys. Lett. B **36**(07), 2150604 (2022)
32. V. Sharma, N. Kant, V. Thakur, Effect of different Gaussian-like laser profiles on electron energy gain in laser wakefield acceleration. Opt. Quantum Electron **56**(1), 45 (2024)
33. H.S. Ghotra, Laser wakefield and direct laser acceleration of electron by chirped laser pulses. Optik (Stuttg) (2022). https://doi.org/10.1016/j.ijleo.2022.169080
34. V.B. Pathak, J. Vieira, R.A. Fonseca, L.O. Silva, Effect of the frequency chirp on laser wakefield acceleration. New J. Phys. **14**(2), 023057 (2012)
35. X. Zhang et al., Effect of pulse profile and chirp on a laser wakefield generation. Phys. Plasmas (2012). https://doi.org/10.1063/1.4714610
36. V. Sharma, S. Kumar, N. Kant, V. Thakur, Effect of frequency chirp and pulse length on laser wakefield excitation in under-dense plasma. Braz. J. Phys. **53**(6), 157 (2023)
37. V. Sharma, S. Kumar, To study the effect of laser frequency-chirp on trapped electrons in laser wakefield acceleration. J. Phys. Conf. Ser. **2267**(1), 012097 (2022)
38. A. Jain, D.N. Gupta, Optimization of electron bunch quality using a chirped laser pulse in laser wakefield acceleration. Phys. Rev. Accel. Beams **24**(11), 111302 (2021)
39. S. Singh, D. Mishra, B. Kumar, P. Jha, Electron acceleration by wakefield generated by the propagation of chirped laser pulse in plasma. Phys. Scr. **98**(7), 075504 (2023)
40. Y. Heydarzadeh, H. Akou, Effect of laser polarization mode on wake wave excitation in magnetized plasma. IEEE Trans. Plasma Sci. **48**(9), 3088–3097 (2020)
41. V. Sharma, S. Kumar, N. Kant, V. Thakur, Enhanced laser wakefield acceleration by a circularly polarized laser pulse in obliquely magnetized under-dense plasma. Opt. Quantum Electron **55**(13), 1150 (2023)
42. X. Zhang, T. Wang, V.N. Khudik, A.C. Bernstein, M.C. Downer, G. Shvets, Effects of laser polarization and wavelength on hybrid laser wakefield and direct acceleration. Plasma Phys. Control Fusion **60**(10), 105002 (2018)
43. V. Sharma, V. Thakur, Lasers wakefield acceleration in underdense plasma with ripple plasma density profile. J. Opt. (2023). https://doi.org/10.1007/s12596-023-01548-5
44. A. Pukhov, I. Kostyukov, Control of laser-wakefield acceleration by the plasma-density profile. Phys. Rev. E **77**(2), 025401 (2008)
45. D.N. Gupta, K. Gopal, I.H. Nam, V.V. Kulagin, H. Suk, Laser wakefield acceleration of electrons from a density-modulated plasma. Laser Part. Beams **32**(3), 449–454 (2014)
46. C. Aniculaesei et al., Electron energy increase in a laser wakefield accelerator using up-ramp plasma density profiles. Sci. Rep. **9**(1), 11249 (2019)
47. W.P. Leemans et al., Electron-yield enhancement in a laser-wakefield accelerator driven by asymmetric laser pulses. Phys. Rev. Lett. **89**(17), 174802 (2002)
48. V. Sharma, S. Kumar, N. Kant, V. Thakur, Excitation of the Laser wakefield by asymmetric chirped laser pulse in under dense plasma. J. Opt. (2023). https://doi.org/10.1007/s12596-023-01326-3
49. B.-S. Xie, A. Aimidula, J.-S. Niu, J. Liu, M.Y. Yu, Electron acceleration in the wakefield of asymmetric laser pulses. Laser Part. Beams **27**(1), 27–32 (2009)
50. K. Gopal, D.N. Gupta, Optimization and control of electron beams from laser wakefield accelerations using asymmetric laser pulses. Phys. Plasmas (2017). https://doi.org/10.1063/1.5001849
51. V. Sharma, S. Kumar, N. Kant, V. Thakur, Effect of wiggler magnetic field on wakefield excitation and electron energy gain in laser wakefield acceleration. Z. Naturfr. A (2023). https://doi.org/10.1515/zna-2023-0238
52. M. Abedi-Varaki, Electron acceleration by a circularly polarized electromagnetic wave publishing in plasma with a periodic magnetic field and an axial guide magnetic field. Mod. Phys. Lett. B **32**(20), 1850225 (2018)
53. K.P. Singh, V.L. Gupta, L. Bhasin, V.K. Tripathi, Electron acceleration by a plasma wave in a sheared magnetic field. Phys. Plasmas **10**(5), 1493–1499 (2003)
54. V. Sharma, S. Kumar, N. Kant, V. Thakur, Enhanced laser wakefield by beating of two co-propagating Gaussian laser pulses. J. Opt. (2023). https://doi.org/10.1007/s12596-023-01250-6
55. N.H. Mohammed, N.E. Cho, E.A. Adegani, T. Bulboaca, Geometric properties of normalized imaginary error function. Stud. Univ. Babes-Bolyai Mat. **67**(2), 455–462 (2022)
56. H.R. Askari, A. Shahidani, Influence of properties of the Gaussian laser pulse and magnetic field on the electron acceleration in laser–plasma interactions. Opt. Laser Technol. **45**, 613–619 (2013)